*Journal of Computer-Aided Molecular Design*, **15:** 145–156, 2001.
*KLUWER/ESCOM*



# Does a diol cyclic urea inhibitor of HIV-1 protease bind tighter than its corresponding alcohol form? A study by free energy perturbation and continuum electrostatics calculations

Lu Wang[a], Yong Duan[a,*], Pieter Stouten[b], George V. De Lucca[b,**], Ronald M. Klabe[b] & Peter A. Kollman[a,***]
[a]*Department of Pharmaceutical Chemistry, University of California, San Francisco, CA 94143-0446, USA*
[b]*DuPont Pharmaceutical Company, DuPont Experimental Station E500, Wilmington, DE 19880-0500, USA*

Received 6 March 2000; Accepted 24 August 2000

*Key words:* continuum electrostatics, cyclic urea inhibitor, DMP323, free energy perturbation, HIV-1 protease, hydroxyl group, pKa

**Summary**

The cyclic urea inhibitors of HIV-1 protease generally have two hydroxyl groups on the seven-membered ring. In this study, free energy perturbation and continuum electrostatic calculations were used to study the contributions of the two hydroxyl groups to the binding affinity and solubility of a cyclic urea inhibitor DMP323. The results indicated that the inhibitor with one hydroxyl group has better binding affinity and solubility than the inhibitor with two hydroxyl groups. Therefore, removal of one hydroxyl group from DMP323 may help to improve the properties of DMP323. This is also likely to be true for other cyclic urea inhibitors. The study also illustrated the difficulty in accurate modeling of the binding affinities of HIV-1 protease inhibitors, which involves many possible protonation states of the two catalytic aspartic acids in the active site of the enzyme.

## Introduction

Human immunodeficiency virus type 1 (HIV-1) [1], the causative agent of Acquired Immunodeficiency Syndrome (AIDS), encodes a 11-kDa protease in the *pol* open reading frame that is responsible for an autoproteolytic release of the protease from the *gag-pol* fusion precursor protein and a subsequent processing of the *gag* and *pol* proteins to yield viral structural proteins and important enzymes for replication, such as reverse transcriptase, endonuclease, and integrase [2, 3]. Since the protease is essential for the maturation of infectious virions, it has emerged as a primary target for the development of therapeutics for the treatment of AIDS [4]. The HIV-1 protease belongs to the aspartic protease family. Like others members of the family, the HIV-1 protease has two catalytic aspartic acids in the active site, and is inactivated by pepstatin [5]. The crystal structures of the free enzyme and of a number of inhibitor complexes have been solved [6, 7]. The enzyme is a dimer composed of two identical polypeptide chains that are associated with a two-fold symmetry (Figure 1). The availability of high resolution crystal structures of both the free protease and a variety of inhibitor complexes has stimulated structure-based design of many highly specific and potent inhibitors of the enzyme [7, 8].

The HIV-1 protease inhibitors can be classified into two categories: peptidomimetics and non-peptidomimetics [7–9]. The peptidomimetic inhibitors are usually transition-state analogs of the protease. Although several peptidomimetic inhibitors such as saquinavir, indinavir and ritonavir [10] have been approved by Federal Drug Administration (FDA) and

*Present adress: Department of Chemistry and Biochemistry, University of Delaware, Newark, DE 19716.
**Questions regarding the synthesis and experimental data of compounds (Table 1) should be addressed to this author; E-mail: George.V.DeLucca.2@dupontpharma.com
***To whom correspondence should be addressed; E-mail: pak@cgl.ucsf.edu

*Figure 1.* The structure of the HIV-1 protease complexed with DMP323 (diol form). Shown in blue and green are the positions of $Asp^{25}/Asp^{25'}$ and $Ile^{50}/Ile^{50'}$ respectively.

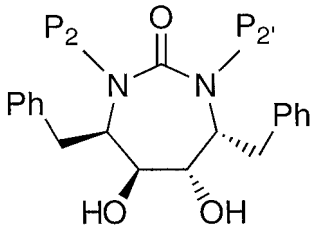


*Figure 2.* The generic form of cyclic urea inhibitors. Ph (phenyl) is at the $P_1$ or $P_{1'}$ position. Ph may be replaced by other groups.

gone into the drug market, the combination of relatively high molecular weight (>600 Dalton), poor solubility and substantial peptide character of peptidomimetic inhibitors have generally resulted in limited oral bioavailability [9]. This has lead to the development of the non-peptidomimetic inhibitors.

Among the non-peptidomimetic inhibitors, the cyclic urea inhibitors [11] are a series of promising inhibitors that are based on a 7-membered cyclic urea scaffold (Figure 2). These inhibitors have nanomolar binding affinities and are orally bioavailable. The inhibitors are bound symmetrically (Figure 2) in the active site of the HIV-1 protease with the urea oxygen accepting two hydrogen bonds from the flap residues $Ile^{50}$ and $Ile^{50'}$. The diol oxygens interact with the two catalytic aspartic acids, $Asp^{25}$ and $Asp^{25'}$. The cyclic urea provides a rigid scaffold for accurate alignment of the key structural elements with their corresponding binding motifs. The rigid scaffold also helps to reduce the large conformational entropy penalties commonly associated with those flexible peptidomimetic inhibitors. The effective hydrogen bonding interactions between the urea oxygen with the flap residues displace the unique structural water commonly observed in the peptidomimetic inhibitor complexes [11].

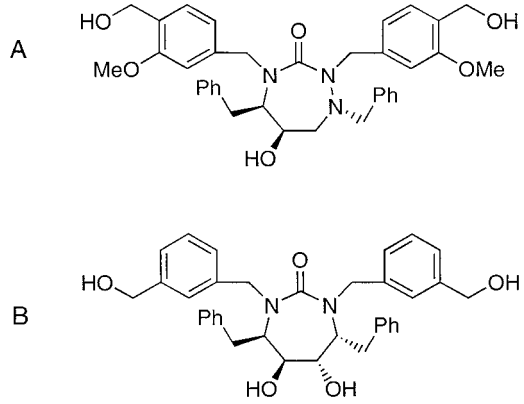


*Figure 3.* (a), A-98881. (b), the cyclic urea inhibitor with a m-(hydroxymethyl)benzyl group at P2 and at P2′ positions.

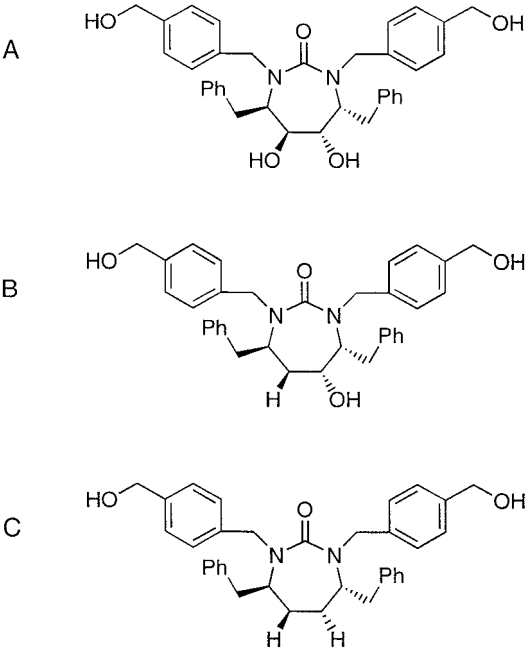


*Figure 4.* The three forms of DMP323 with none ('desoxy'), one ('alcohol') and two ('diol') hydroxyl groups on the seven-membered ring.

A prominent feature of the cyclic urea inhibitors is that they usually have two hydroxyl groups on the 7-membered ring. In the original design [11], the two hydroxyl groups were introduced to maximize hydrogen bonding interactions with the two catalytic aspartic acids. However, we observed that A-98881 (Figure 3a), a variant of cyclic urea inhibitors has only one hydroxyl group on its 7-membered ring but has a $K_1$ of 5 pM, and binds more tightly than any re-

*Table 1.* $K_i$ (nM) of cyclic urea analogs

| P2/P2′ (see Figure 2) | Diol | Alcohol | Desoxy |
|---|---|---|---|
| p-Hydroxymethylbenzyl | 0.34 | – | 250 |
| m-Hydroxymethylbenzyl | 0.14 | 0.058 | 170 |
| Benzyl | 3.0 | 3.0 | – |
| Cyclopropylmethyl | 2.8 | 6.4 | – |

ported cyclic urea inhibitors [12]. This indicates that the second hydroxyl group may be unnecessary for tight binding. A diol compound, DMP323 (Figure 4), a representative cyclic urea inhibitor, was found unsuccessful in clinical trials due to its low aqueous solubility which leads to highly variable human oral bio-availability [11]. The diol DMP323 may not have a better solubility than its corresponding alcohol form due to possible intramolecular hydrogen binding interactions between the two hydroxyl groups. Therefore, removing one hydroxyl group of DMP323 may help to improve its solubility. For all these reasons, it is of interest to study the contributions of the hydroxyl groups of a cyclic urea inhibitor to its binding affinity as well as to solubility.

The binding affinity differences of DMP323 were studied with two, one and none hydroxyl groups on its 7-membered ring by free energy perturbation and continuum electrostatics calculations. The three forms of DMP323 were named as 'diol', 'alcohol' and 'desoxy', respectively (Figure 4). The experimental $K_1$ for these three species with different P2/P2′ substitutes are reported in Table 1. We found that the alcohol form has considerably higher binding affinity and solubility than the desoxy form. However, the diol form does not have higher binding affinity and solubility than the alcohol form. This suggests that removal of one hydroxyl group on the 7-membered ring may be helpful to improve the properties of DMP323. This may help to improve the properties of other cyclic urea inhibitors in general because similar interactions with the HIV-1 protease are involved.

## Materials and methods

### *Model, parameters and MD simulations*

The structure of HIV-1 protease complexed with DMP323 was obtained from Brookhaven Protein Data Bank (PDB code: 1BVE). The protease consists of two sub-units with identical sequences of 99 residues (1–99 and 1′–99′). The structures of the alcohol or desoxy forms were model built based on the complex structure of DMP323 using standard geometry.

For the simulations on the complexes, a 20-Å cap of TIP3P water [13] molecules centered at the center of mass of each inhibitor was used. The systems were neutralized by adding counterions. For the dianionic state, 8 counterions ($Na^+$ or $Cl^-$) were placed around residues $Glu^{21}$, $Arg^{41}$, $Lys^{45}$, $Lys^{55}$, $Glu^{21'}$, $Arg^{41'}$, $Lys^{45'}$, $Lys^{55'}$, one additional counterion was placed around residue $Lys^{14'}$ for the singly protonated state; two additional counterions were placed around residues $Lys^{14}$ and $Lys^{14'}$, respectively, for the doubly protonated state. All counterions were far away from the $Asp^{25}$ and $Asp^{25'}$ sites. Most of ions were far away from the binding sites and remained in the vicinity of the side chains that they were initially placed next to. Only residues within the sphere and the cap water molecules were allowed to move in the molecular dynamics simulations. Each system consists of about 1000 protein atoms and 390 water molecules. The cap water molecules were kept from escaping by a weak harmonic restraining potential of 1.5 kcal/mol/Å$^2$ at the surface of the dynamic sphere. Prior to free energy simulations, each system was energy minimized for 500 steps and equilibrated for 10 ps by molecular dynamics simulations. For the simulations in water, each inhibitor was placed at the center of a box of $37x37x37$ Å$^3$ filled with $\sim$ 1500 TIP3P water molecules under standard conditions. Though the different treatments on the boundary conditions (CAP vs box) can introduce additional systematic errors to the calculations of binding free energies, the thermodynamic cycle, discussed below, effectively eliminates that error since only $\Delta\Delta G$ (i.e., the binding free energy difference) is calculated. This holds true so long as the boundary conditions remain the same during the 'mutation', which is the case in the present study. This, once again, shows the advantage of free energy perturbation method.

All MD simulations and energy minimizations were performed with AMBER4.1 program [14] with the all atom force field developed by Cornell *et al.* [15]. The van der Waals (VDW), bond, bond angle, and dihedral angle (BADH) parameters of the amino acids and the inhibitors as well as the partial charges of the amino acids were taken from the AMBER4.1 database. To obtain the atomic charges of the inhibitors, each inhibitor was divided into three pieces: a piece with a hydroxylmethyl benzyl group, a piece with a

benzyl group, and a piece with the central 7-membered ring. Every carbon atom connecting two moieties was assigned to both pieces and changed to a $CH_3$ group. For the diol (DMP323), alcohol and desoxy forms, the only differences are in the piece with the 7-membered ring. The atomic charges of each piece were obtained by fitting the electrostatic potentials around the piece with the RESP method [16]. The electrostatic potential was obtained by a single point *ab initio* quantum mechanical calculation with 6–31G* basis set using Gaussian 94 [17] on a geometry generated by energy minimization with the AM1 method. The charges of the buffer carbon atoms connecting the moieties and those of the hydrogen atoms attached to them were adjusted for each inhibitor to ensure the neutrality of the inhibitors.

The simulations were performed with a time step of 2 femtoseconds (fs) and with a cutoff radius of 8 Å for the non-bonded interactions. The bond lengths were constrained to their equilibrium values using the SHAKE and the SETTLE algorithms [18, 19]. The temperature was maintained at 300 K by coupling of the system to a heat bath [20]/ For the simulations in water, periodic boundary conditions were applied and the pressure was maintained at 1 atm by adjustment of the volume of the periodic box [20].

*Thermodynamic cycles*

The following thermodynamic cycle was used to assess the binding free energy difference of two inhibitors, $L_1$ and $L_2$:

$$\begin{array}{ccccc} & & & \xrightarrow{\Delta G_{b1}} & \\ L_1 & + & P & \longrightarrow & L_1P \\ & \Delta_{Gms}\downarrow & & & \downarrow\ \Delta G_{mp} \\ L_1 & + & P & \longrightarrow & L_2P \\ & & & \xrightarrow{\Delta G_{b2}} & \end{array} \qquad (1)$$

where P stands for the HIV-1 protease; $\Delta G_{b1}$ and $\Delta G_{b2}$ are the binding free energies of $L_1$ and $L_2$; $\Delta G_{mp}$ and $\Delta G_{ms}$ are the mutational free energies of $L_1 \rightarrow L_2$ in the complex and in solution, respectively. Because free energy is a state function, the free energies are related by the following equations:

$$\Delta\Delta G_{bind} = \Delta G_{b2} - \Delta G_{b1} = \Delta G_{mp} - \Delta G_{ms} \qquad (2)$$

where $\Delta\Delta G_{bind}$ is the difference in binding free energy between $L_1$ and $L_2$. Recent developments have made it possible to obtain the qualitative binding free energies using either an empirical method developed by Aqvist and co-workers [21, 22] or methods based on continuum solvent electrostatics such as MM/PB-SA [23] or MM/GB-SA [24]. However, direct accurate computations of $\Delta G_{b1}$ and $\Delta G_{b2}$ are difficult due to possible large conformational changes in the binding processes. Fortunately, $\Delta G_{mp}$ and $\Delta G_{ms}$ can be readily calculated by the free energy perturbation method in molecular dynamics simulations.

To calculate the solvation free energy difference between two ligands, $L_1$ and $L_2$, the following thermodynamic cycle was used:

$$\begin{array}{ccc} & \xrightarrow{\Delta G_{s1}} & \\ L_1\ \text{(vacuo)} & \rightarrow & L_1\ \text{(solution)} \\ \Delta G_{mv}\downarrow & & \downarrow\ \Delta G_{ms} \\ L_2\ \text{(vacuo)} & \rightarrow & L_2\ \text{(solution)} \\ & \xrightarrow{\Delta G_{s2}} & \end{array} \qquad (3)$$

where $\Delta G_1$ and $\Delta G_2$ are the solvation free energies of $L_1$ and $L_2$. $\Delta G_{mv}$ is the mutational free energy of $L_1 \rightarrow L_2$ *in vacuo* ($\Delta G_{ms}$ is the same as that in Equation). The solvation free energy difference was calculated as

$$\Delta\Delta G_{solv} = \Delta G_{s2} - \Delta G_{s1} = \Delta G_{ms} - \Delta G_{mv} \qquad (4)$$

where $\Delta\Delta G_{solv}$ is the difference in solvation free energy between $L_1$ and $L_2$.

*Free energy simulations*

The thermodynamic integration method [25] was used to calculate free energy changes. In the method, for the transformation of one thermodynamic state into another, a coupling parameter $\lambda$ is introduced and the Hamiltonian of the two states are defined as $H_0$ ($\lambda = 0$) and $H_1$ ($\lambda = 1$) The total free energy change for the transformation is expressed as the following integral

$$\Delta G = \int_0^1 \langle \partial H(\lambda)/\partial\lambda \rangle_\lambda \, d\lambda \qquad (5)$$

where $\langle \partial H(\lambda)/\partial\lambda \rangle_\lambda$ is an ensemble average at $\lambda$. In practice, a number of evenly-spaced windows with different $\lambda$ values ranging from 0 to 1 are chosen and $\langle \partial H(\lambda)/\partial\lambda \rangle_\lambda$ is calculated by averaging over molecular dynamics trajectories at each window. Usually, the contributions from kinetic energy change can be neglected due to constant temperature and $\Delta G$ is approximated by

$$\Delta G \approx \sum_i \langle \partial V(\lambda)/\partial\lambda \rangle_{\lambda i} \Delta\lambda \qquad (6)$$

where $\lambda_i$ is the $\lambda$ value of the $i$th window and $\Delta\lambda$ is the interval between successive windows. $V$ is the potential function that describes the atomic interactions in the system.

Free energy simulations were carried for all possible protonation states of $Asp^{25}$ and $Asp^{25'}$ in the HIV-1 protease and are illustrated by the following binding equilibrium diagram:

$$\begin{array}{ccccccc}
 & & \overset{\Delta G_{b1}}{} & & \overset{\Delta G_{b2}}{} & & \overset{\Delta G_{b3}}{} \\
N + P^{2-} + 2H^+ & \longrightarrow & NP^{2-} + 2H^+ & \longrightarrow & NP^{2-}H^+ + H^+ & \longrightarrow & NP^{2-}H^+H^+ \\
\Delta G_{m1} \downarrow & & \downarrow \Delta G_{m2} & & \downarrow \Delta G_{m3} & & \downarrow \Delta G_{m4} \\
 & & \overset{\Delta G_{b4}}{} & & \overset{\Delta G_{b5}}{} & & \overset{\Delta G_{b6}}{} \\
M + P^{2-} + 2H^+ & \longrightarrow & MP^{2-} + 2H^+ & \longrightarrow & MP^{2-}H^+ + H^+ & \longrightarrow & MP^{2-}H^+H^+ \\
\Delta G_{m5} \downarrow & & \downarrow \Delta G_{m6} & & \downarrow \Delta G_{m7} & & \downarrow \Delta G_{m8} \\
 & & \overset{\Delta G_{b7}}{} & & \overset{\Delta G_{b8}}{} & & \overset{\Delta G_{b9}}{} \\
D + P^{2-} + 2H^+ & \longrightarrow & DP^{2-} + 2H^+ & \longrightarrow & DP^{2-}H^+ + H^+ & \longrightarrow & DP^{2-}H^+H^+
\end{array} \qquad (7)$$

where 'D', 'M', 'N' stand for the 'diol', 'alcohol' and 'desoxy' inhibitors, respectively, $P^{2-}$, $P^{2-}$ $H^+$ and $P^{2-}H^+H^+$ represent the dianionic, singly protonated and doubly protonated states of the HIV-1 protease. The $\Delta G$'s in the horizontal direction are the free energy changes associated with binding of the inhibitors to the protease with different protonation states and those in the vertical direction are the free energy changes of mutations of one inhibitor into another in solution or in the complexes with the same protonation state. The horizontal $\Delta G$ difference of two inhibitors can be expressed as the vertical $\Delta G$ difference of the two inhibitors. For example, $\Delta G_{b4} - \Delta G_{b1} = \Delta G_{m2} - \Delta G_{m1}$ and $\Delta G_{b5} - \Delta G_{b2} = \Delta G_{m3} - \Delta G_{m2}$. In the study, only the vertical $\Delta G$'s were calculated for the reasons stated above. The possibility of the inhibitors' binding to the protease with different protonation states was investigated by continuum electrostatics calculations that estimated the $pK_a$'s of the two catalytic aspartic acids in the complexes.

The calculations of the solvations free energy differences of the inhibitors are illustrated by the following diagram:

$$\begin{array}{ccccc}
 & \overset{\Delta G_{m1'}}{} & & \overset{\Delta G_{m5'}}{} & \\
N\ (vacuo) & \longrightarrow & M\ (vacuo) & \longrightarrow & D\ (vacuo) \\
\Delta G_{s1} \downarrow & & \Delta G_{s2} \downarrow & & \Delta G_{s3} \downarrow \\
N\ (solution) & \longrightarrow & M\ (solution) & \longrightarrow & D\ (solution) \\
 & \underset{\Delta G_{m1}}{} & & \underset{\Delta G_{m5}}{} &
\end{array} \qquad (8)$$

where $\Delta G_{m1}$ and $\Delta G_{m5'}$ are the mutational free energies of N $\rightarrow$ M and M $\rightarrow$ D. $\Delta G_{m1}$ and $\Delta G_{m5}$ are the same as those in Equation 7. $\Delta G_{s1}$, $\Delta G_{s2}$, and $\Delta G_{s3}$ are the solvation free energies of N, M, D, respectively. Similarly, according to the principle of thermodynamic cycles, $\Delta G_{s2}$ - $\Delta G_{s1}$ = $\Delta G_{m1}$ - $\Delta G_{m1}$ and $\Delta G_{s3}$ - $\Delta G_{s2}$ = $\Delta F_{m5}$ - $\Delta G_{m5'}$.

The single topology method was used for the free energy calculations, in which the two molecular states were represented in one topology structure and in the free energy calculations, the parameters of the molecule were changed gradually from those of one state to another. The mutations of N $\rightarrow$ M and M $\rightarrow$ D both involve the introduction of one hydroxyl group, or the transformation of a hydrogen into a hydroxyl group. The bond length of C-H was changed to that of C-O in the calculations. The contribution to the free energies due to the change of bond length needs to be included [26, 27] and were calculated by the potential of mean force (PMF) algorithm [27]. The contributions of intra-perturbed group may not be negligible. Therefore, we included all the intra-perturbed group contributions in the calculations. Each free energy calculation consisted of a 324 ps forward simulation from $\lambda = 1$ to 0 and a 324 ps backward simulation from $\lambda = 0$ to 1. The number of windows was 81 and in each window, 2 ps was used for equilibration and 2 ps for sampling. The average of the forward and backward changes was taken as the estimated free energy change. The difference between the forward and the backward changes is the hysteresis of the calculation.

For qualitative purposes, the free energy changes were decomposed into the contributions from electrostatic (EL) and van der Waals (VDW) interactions, bonds, bond angles and dihedrals (BADH) by decomposing $\langle \partial H(\lambda)/\partial\lambda \rangle_\lambda$ at each $\lambda$ into the contributions from different interactions, as described in previous studies from this laboratory [28, 29]. This is possible because $\partial V(\lambda)/\partial\lambda$ can be expressed as a sum of contributions from different interactions. According to Equation 2, for two inhibitors, $\Delta\Delta G_{bind} = \Delta G_{mp} - \Delta G_{ms}$. Therefore, the differential contribution of each term to $\Delta G_{mp}$ and $\Delta G_{ms}$ gives the contribution of that term to the $\Delta\Delta G_{bind}$ of the two inhibitors. Similarly, according to Equation 4, for two inhibitors, $\Delta\Delta G_{solv} = \Delta G_{ms} - \Delta G_{mv}$ and therefore, the differential contribution of each term to $\Delta G_{ms}$ and $\Delta G_{mv}$ gives the contribution of that term to the $\Delta\Delta G_{solv}$ of the two inhibitors. We shall note, however, the analysis described above can only serve qualitative purposes since only the free energy is a state function and the individual components are not state functions and are path-dependent [30].

*Continuum electrostatics calculations*

The continuum electrostatics calculations were used to estimate the $pK_a$'s of the two catalytic aspartic acids in the inhibitor complexes. Since the experimental $pK_a$'s of the two aspartic acids in the free protease are available [31], to obtain their $pK_a$'s in the inhibitor complexes, we only need to estimate the $pK_a$ shifts in the complexes. The protonation equilibrium of two aspartic acids of the protease in the presence of an inhibitor is the following:

$$\begin{array}{ccccc} & \overset{K_{a2}}{} & & \overset{K_{a1}}{} & \\ L + P^{2-} + 2H^+ & \longleftarrow & L + P^{2-}H^+ + H^+ & \longleftarrow & L + P^{2-}H^+H^+ \\ K_{i2} \downarrow & & K_{i1} \downarrow & & K_{i0} \downarrow \\ LP^{2-} + 2H^+ & \longleftarrow & LP^{2-}H^+ + H^+ & \longleftarrow & LP^{2-}H^+H^+ \\ & \underset{K_{a2'}}{} & & \underset{K_{a1'}}{} & \end{array} \tag{9}$$

where $K_{a1}$, $K_{a2}$ and $K_{a1'}$, $K_{a2'}$ are the proton dissociation constants in the free protease and in the inhibitor complex. $K_{i0}$, $K_{i1}$, and $K_{i2}$ are the equilibrium constants of binding of the inhibitor to the doubly protonated, singly protonated, and dianionic states of the protease. The $pK_a$ shifts are expressed as

$$\Delta pK_{a1} = pK_{a1'} - pK_{a1} = (\Delta G_{a1'} - \Delta G_{a1})/(2.303 \times k_B T) \tag{10}$$

$$\Delta pK_{a2} = pK_{a2'} - pK_{a2} = (\Delta G_{a2'} - \Delta G_{a2})/(2.303 \times k_B T) \tag{11}$$

where $k_B$ is the Boltzmann's constant and T is the temperature. The $\Delta G$'s are the free energy changes corresponding to the $K_a$'s. It is easy to see that the above two free energy differences can be further expressed as

$$\Delta G_{a1'} - \Delta G_{a1} = [G(LP^{2-}H^+) - G(LP^{2-}H^+H^+)] - [G(P^{2-}H^+) - G(P^{2-}H^+H^+)] \tag{12}$$

$$\Delta G_{a2'} - \Delta G_{a2} = [G(LP^{2-}) - G(LP^{2-}H^{)}] - [G(P^{2-}) - G(P^{2-}H^+)] \tag{13}$$

where G represents absolute free energy. It is difficult to accurately calculate the free energy differences in each bracket because they involve calculations of small differences between two large free energy numbers. Instead, we approximated each free energy difference in the brackets by the difference in the electrostatic interaction energy of the aspartic acid with the surrounding environment in two protonation states. The electrostatic interaction energies of the aspartic acid with the surrounding environment in the two protonation states were calculated by the continuum electrostatics method, in which the electric field around a molecule in solution satisfies the linearized Poisson–Boltzmann equation [32].

$$\nabla(\varepsilon(x)\nabla\phi(x)) - \kappa^2\phi(x) + 4\pi\rho(x) = 0 \tag{14}$$

where $\phi$ is the electric potential, $\varepsilon$ is the dielectric constant, $p$ is the fixed charge density and $\kappa$ is the modified Debye–Hückel parameter which depends on the ionic strength and temperature of the solution. The Poisson–Boltzmann equation can be solved numerically by the finite difference method, in which the continuous functions are approximated by distinct values at points on a cubic grid [32]. The electrostatic interaction between a group of atoms (such as an aspartic acid) with the surrounding environment is [32]

$$\Delta E = \tfrac{1}{2}\sum \phi_i q_i \tag{15}$$

where $\phi_i$ is the potential on the $i$th charge $q_i$ of the group of atoms. It is noted that in calculating the $pK_a$ shifts of the two catalytic aspartic acids of the HIV-1 protease, we assume that the protonation states of other titratable groups are the same. This is appropriate because we are only interested in the $pK_a$ shifts of the two aspartic acids.

The Poisson–Boltzmann calculations were performed with the Delphi package [33, 34], using a dielectric constant of $\varepsilon_p = 4$ or 20 for the protein and a dielectric constant of $\varepsilon_w = 78.5$ for the solution. $\varepsilon_p = 20$ was used because it was suggested this gives better results for $pK_a$'s than $\varepsilon_p = 4$ [35]. The ionic strength of the solution was chosen to be 0.15 M. The calculations were performed on the HIV-1 protease and its cyclic urea inhibitor complexes for different protonation states of the two aspartic acids. To accurately calculate the electric potential, for each case, a two-step focussing calculation [33] with the grid sizes of 1 Å and 0.5 Å was performed.

*Table 2.* The calculated free energy changes (in kcal/mol)[a]

| | Desoxy → Alcohol | | | Alcohol → Diol | | |
|---|---|---|---|---|---|---|
| | fwd[c] | bwd[c] | ave | fwd[c] | bwd[c] | ave |
| *In vacuo* | −4.6 | −4.5 | −4.5 | 6.1 | 6.2 | 6.2 |
| in water | −9.0 | −9.0 | −9.0 | 8.1 | 7.6 | 7.8 |
| **protease** | | | | | | |
| Dianionic | −16.0 | −12.4 | −14.2 | 10.0 | 9.9 | 10.0 |
| Single H | | | | | | |
| 25′-$O_2$ | −6.8 | −6.3 | −6.5 | 8.2 | 11.7 | 10.0 |
| 25′-$O_1$ | −9.8 | −9.1 | −9.4 | 7.7 | 7.4 | 7.6 |
| 25-$O_2$ | −10.6 | −10.2 | −10.4 | 8.4 | 8.5 | 8.5 |
| 25-$O_1$ | −11.8 | −11.4 | −11.6 | 10.2 | 10.0 | 10.1 |
| Double Hs | | | | | | |
| 25-$O_2$, 25′-$O_2$ | −6.6 | −7.9 | −7.2 | 11.4 | 12.9 | 12.1 |
| 25-$O_1$, 25′-$O_2$ | −11.7 | −11.1 | −11.4 | 10.4 | 11.0 | 10.7 |
| 25-$O_2$, 25′-$O_1$ | −12.6 | −6.2 | −9.4 | 9.1 | 8.8 | 9.0 |
| | −10.0 | −6.5 | −8.3[b] | | | |
| | −7.1 | −10.4 | −8.8[b] | | | |
| | −11.2 | −6.3 | −8.8[b] | | | |
| 25-$O_1$, 25′-$O_1$ | −11.4 | −11.9 | −11.6 | 9.9 | 10.6 | 10.3 |

[a]'fwd', 'bwd', 'ave' denote forward, backward and average free energy changes. Each free energy calculation used 81 windows with 2 ps/2 ps for equilibration and sampling. '25-$O_1$', '25-$O_2$', '25′-$O_1$', '25′-$O_2$' are the protonation positions.
[b]These entries were calculated using slightly different starting structures with 101 windows and 2.4 ps/2.6 ps for equilibration and sampling.
[c]The forward and backward free energies are given here as an estimation of the margin of error associated with the calculation.

## Results

### *Estimation of the solvation and binding free energy differences of the inhibitors from free energy calculations*

The calculated free energy changes for the mutations of desoxy→alcohol and alcohol→diol *in vacuo*, in water and in the inhibitor complexes are listed in Table 2. For both the singly protonated and the double protonated states of the protease, there are four possible protonation positions on the two aspartic acids. The free energy calculations were performed for all possible protonation positions. The differences in solvation and binding free energies of the ligands were estimated using Equations 2 and 4 (Tables 3 and 4).

Solvation free energies were calculated using gas phase as the reference state, since the structure in the crystalline state, which is a more proper medicinal chemical reference state, is not available. For desoxy→alcohol, the solvation free energy decreases by 4.5 kcal/mol, indicating an increase in solubility.

*Table 3.* The calculated solvation free energy changes ($\Delta\Delta G_{solv}$) of Desoxy → Alcohol and Alcohol → Diol (in kcal/mol)

| | Desoxy → Alcohol | Alcohol → Diol |
|---|---|---|
| $\Delta\Delta G_{solv}$ | −4.5 | +1.6 |

But the estimated solvation free energy appears to be reasonable because the contribution of a hydroxyl group to solvation free energies is about −5 kcal/mol [36]. It is interesting that for alcohol→diol, the solvation free energy increases by 1.6 kcal/mol, indicating a decrease in solubility. The estimated reduced solubility of the diol inhibitor compared with the alcohol inhibitor could be caused by intramolecular hydrogen binding between the two hydroxyl groups. To check this possibility, we calculated the average O-H distance and O-H-O angle between the two hydroxyl groups from a 200 ps simulation of the diol inhibitor *in vacuo*. The O-H distance was estimated to be 2.8 ±

*Table 4.* The calculated binding free energy changes ($\Delta\Delta G_{bind}$) of Desoxy→ Alcohol and Alcohol→ Diol (in kcal/mol)

| Protonation states | Desoxy→ Alcohol | Alcohol → Diol | Desoxy → Diol |
|---|---|---|---|
| Dianionic | −5.2 | +2.2 | −3.0 |
| Single H | | | |
| 25′-$O_2$ +2.4 | +2.2 | +0.2 | |
| 25′-$O_1$ | −0.4 | −0.2 | −0.6 |
| 25-$O_2$ | −1.4 | +0.6 | −0.8 |
| 25-$O_1$ | −2.6 | +2.3 | −0.3 |
| Double Hs | | | |
| 25-$O_2$, 25′-$O_2$ | +1.8 | +4.4 | +6.2 |
| 25-$O_1$, 25′-$O_1$ | −2.4 | +2.9 | +0.5 |
| 25-$O_2$, 25′-$O_1$ | −0.4 | +1.2 | +0.8 |
| 25-$O_1$, 25′-$O_1$ | −2.6 | +2.5 | −0.1 |
| Experiments | | | |
| DMP323 (Desoxy → Diol) | | | −4.0 |
| [a] | −4.8 | +0.5 | −4.3 |

[a]The results for the cyclic inhibitor with a m-(hydroxymethylbenzyl) group at $P_2$ and at $P_2^{'}$ positions.

0.6 Å and the O-H-O angle was calculated to be 73 ± 36°. Both the distance and angle are not favorable for hydrogen bonding. This is because the two hydroxyl groups are on different sides of the seven-membered ring (Figure 2). Therefore, the lower solubility of the diol form than the alcohol form can not be explained by intramolecular hydrogen bonding. A plausible explanation may be that in the diol form, the two OH groups can interfere with each other in forming hydrogen bonds with water molecules because the oxygen of one OH has repulsive electrostatic interactions with those water molecules forming hydrogen bonds with another OH group. As a result, the solvation of the diol form may not be as effective as the alcohol form.

The calculated binding free energy differences of the inhibitors depend on the protonation states and protonation positions of the protease. For the dianionic state, the estimated $\Delta\Delta G_{bind}$ of desoxy→alcohol is −5.2 kcal/mol and the estimated $\Delta\Delta G_{bind}$ of alcohol→diol is +2.2 kcal/mol. Thus, the alcohol form binds tighter than the diol form, which binds tighter than the desoxy form. For the singly and doubly protonated states, the trend depends on the protonation positions of the catalytic aspartic acids. However, for most cases, the estimated $\Delta\Delta G_{bind}$ of desoxy→alcohol is negative and the estimated $\Delta\Delta G_{bind}$ of alcohol→diol is positive. It is very likely that the alcohol form has the highest binding affinity to the singly and doubly protonated states.

While the experimentally determined binding affinity for the alcohol form of DMP323 is not currently available, the data for the desoxy form is listed in Table 1 (P. Stouten, G.V. De Lucca, and R.M. Klabe, unpublished data). The data for the diol, alcohol, and desoxy forms of the closely related m-hydroxymethyl analog (Figure 3b) is available and is also listed in Table 1 for comparison with the simulation results. These results have been converted into free energies and are given in Table 4. The experimental data (Table 1) suggests that the free energy differences may be dependent on the P2 substituent, since in the case of the benzyl P2 group there is no difference in binding affinity between diol and alcohol forms. In the case of the cyclopropylmethyl P2 group, the diol has a better binding affinity than the alcohol form. However, due to the high-degree of similarity between DMP323 and the m-hydroxymethyl analog, we expect that a similar trend might be shared by both DMP323 and the m-hydroxymethyl analog. Indeed, for the m-hydroxymethyl analog, $\Delta\Delta G_{bind}$ of desoxy→diol is −4.3 kcal/mol, very close to that of DMP323, −4.0 kcal/mol (Tables 1 and 4). Furthermore, for the m-hydroxymethyl analog, $\Delta\Delta G_{bind}$ of desoxy→alcohol is −4.8 kcal/mol and $\Delta\Delta G_{bind}$ of alcohol→diol is +0.5 kcal/mol (Table 4). This

*Table 5.* The estimated pKa's of $Asp^{25}$ and $Asp^{25'}$ in the HIV-1 protease-inhibitor complexes[a]

| Complexes | | $\varepsilon_p = 4$ | | $\varepsilon_p = 20$ | |
|---|---|---|---|---|---|
| | | $pK_{a1}$ | $pK_{a2}$ | $pK_{a1}$ | $pK_{a1}$ |
| Diol | 25-$O_2$, 25′-$O_2$ | 7.5 | 12.5 | 4.6 | 6.7 |
| | 25-$O_1$, 25′-$O_2$ | 7.0 | 12.9 | 4.7 | 6.8 |
| | 25-$O_2$, 25′-$O_2$ | 7.8 | 11.9 | 4.8 | 6.7 |
| | 25-$O_1$, 25′-$O_1$ | 6.8 | 12.4 | 4.8 | 6.7 |
| Alcohol | 25-$O_2$, 25′-$O_2$ | 8.9 | 12.1 | 5.0 | 6.6 |
| | 25-$O_1$, 25′-$O_2$ | 9.0 | 12.0 | 4.9 | 6.6 |
| | 25-$O_2$, 25′-$O_1$ | 10.5 | 12.0 | 5.2 | 6.6 |
| | 25-$O_1$, 25′-$O_1$ | 10.7 | 11.9 | 5.3 | 6.6 |
| Desoxy | 25-$O_2$, 25′-$O_2$ | 8.6 | 13.4 | 4.2 | 6.5 |
| | 25-$O_1$, 25′-$O_1$ | 9.8 | 13.8 | 4.8 | 6.9 |
| | 25-$O_2$, 25′-$O_2$ | 10.2 | 12.8 | 4.4 | 6.4 |
| | 25-$O_1$, 25′-$O_1$ | 11.4 | 13.3 | 5.2 | 6.8 |

[a]For each complex, the $pK_a$s were calculated for four possible protonation positions: (25-$O_2$, 25′-$O_2$), (25-$O_1$, 25′-$O_2$), (25-$O_2$, 25′-$O_1$), (25-$O_1$, 25′-$O_1$). For the free enzyme, $pK_{a1}$ = 3.1–3.7, $pK_{a2}$ = 4.9–6.5 [31, 37].

suggests that the alcohol form may also have a better binding affinity than the diol form for DMP323. Therefore, our simulation results are qualitatively consistent with the experimental measurements, which suggest that the alcohol form has a better binding affinity than the diol form.

*Analysis of the protonation states and protonation positions of the protease in the inhibitor complexes by continuum electrostatics calculations*

In our free-energy simulations, we assumed that the three forms of inhibitors bind to the protease with the same protonation state or protonation position. This may not be true. To determine the protonation state and position of the protease, we carried out continuum electrostatics calculations. In the free HIV-1 protease, the measured $pK_a$'s of the two catalytic aspartic acids were $pK_{a1}$ = 3.1-3.7 and $pK_{a2}$ = 4.9–6.5 [31, 37]. Based on the calculated $pK_a$ shifts in the inhibitor complexes, the $pK_a$'s of the two aspartic acids in the complexes were estimated using Equations 10 and 11 (Table 5).

For all the complexes, the estimated $pK_a$'s are higher than those in the free enzyme, indicating that extractions of the protons in the complexes are more difficult than in the free enzyme. Since the binding affinity of DMP323 was measured at pH = 5.5 the dianionic state of the protease seems to be unlikely for the three inhibitors. The calculated $pK_a$'s strongly depend on the dielectric constant of the protein interior, $\varepsilon_p$: the estimated $pK_a$'s with $\varepsilon_p = 4$ are much larger than those estimated with $\varepsilon_p = 20$. This makes if difficult to determine the exact protonation state because for $\varepsilon_p = 4$, the protease is predicted to be doubly protonated; for $\varepsilon_p = 20$, the protease is predicted to be singly protonated. Based on the catalysis mechanism of the aspartic protease family and theoretical studies, it is generally expected that one of the two aspartic acids is protonated and the other is charged [5, 37–44]. A recent measurement of the effective dielectric constant in the hydrophobic core of staphylococcal nuclease gave $\varepsilon_p$ = 10–12 [45]. In light of the polar character of the active site of the HIV-1 protease, its dielectric constant may be higher. This evidence suggests that the protease is singly protonated, consistent with theoretical study based on the linear approximation method [22]. However, a NMR study using chemical shift titrations and H/D isotope shift measurement suggested that the protease is doubly protonated in the DMP323 complex in the pH range of 2–7 [46].

Although we are not able to exactly determine the protonation states of the inhibitor complexes due to the uncertainty in choosing $\varepsilon_p$, we may comment on the following two questions based on the binding free energy results and the estimated $pK_a$'s. First, are the three inhibitor complexes in the same protonation state? It is very likely that they are in the same protonation state. This is because if the $pK_{a1}$'s of the complexes are all larger than 5.5, they will be all in the doubly protonated state. If their $pK_{a1}$'s are below or around 5.5, as in the case of $\varepsilon_p = 20$, their $pK_{a1}$'s will be very close to each other, and they will be all in the singly protonated state. Second, if the three complexes are in the same protonation state, do they have the same protonation position? This is a more difficult question to answer given the accuracy of the current continuum electrostatics calculations. For $\varepsilon_p = 20$, which corresponds to the singly protonated state of the complexes, different protonation positions make small differences in binding free energies because the estimated $pK_{a2}$'s are similar for different protonation positions of each complex. For $\varepsilon_p = 4$, which corresponds to the doubly protonated state of the complexes, different protonation positions have significantly different $pK_{a1}$'s and $pK_{a2}$'s. The most likely protonation position is the one that has the largest sum of $pK_{1a}$ and $pK_{a2}$. For the diol, al-

cohol and desoxy complexes, the possible protonation positions are (25-$O_2$, 25′-$O_2$), (25-$O_1$, 25′-$O_1$) and (25-$O_1$, 25′-$O_1$). The alcohol and desoxy complexes have the same protonation position of (25-$O_1$, 25′-$O_1$). According to Table 4, $\Delta\Delta G_{bind} = -2.6$ kcal/mol for desoxy→alcohol. The alcohol and diol complexes are in different protonation positions. If the diol complex is in the protonation position of (25-$O_1$, 25′-$O_1$), $\Delta\Delta G_{bind} = +2.5$ kcal/mol for alcohol→diol. The free energy difference between (25-$O_2$, 25′-$O_2$) and (25-$O_1$, 25′-$O_1$) in the diol complex is 0.8 $pK_a$ unit, or 0.8 x 1.4 = 1.1 kcal/mol. Including this contribution, for alcohol→diol, $\Delta\Delta G_{bind} = 2.5 - 1.1 =$ 1.4 kcal/mol. A similar calculation can be performed using the calculated $\Delta\Delta G_{bind}$ for alcohol→diol in the protonation position of (25-$O_2$, 25′-$O_2$). The result is $\Delta\Delta G_{bind} = 2.2$ kcal/mol for alcohol→diol. Therefore, when the protonation positions of the complexes are considered, the conclusion that the alcohol form has the highest binding affinity is not changed.

## Discussion

In this study, we studied the binding affinities of the diol, alcohol and desoxy forms of DMP323 by free energy perturbation and continuum electrostatics calculations. It was found that the estimated solubility and binding affinity of the alcohol inhibitor are higher than that of the desoxy inhibitor, but neither the estimated solubility nor the estimated binding affinity of the diol inhibitor are higher than those of the alcohol inhibitor. The predicted trend in binding affinities of the inhibitors is consistent with the experimental measurements on the cyclic urea inhibitor with a m-(hydroxymethyl)benzyl group at $P_2$ and $P_2'$ positions. For DMP323, the alcohol inhibitor may be able to overcome the problems of low solubility of the diol inhibitor without losing its binding affinity. We anticipate that a similar trend is observed for other cyclic urea inhibitors.

To understand the energetic basis of the solvation and binding free energy differences of the inhibitors, we decomposed the calculated $\Delta\Delta G_{solv}$'s and $\Delta\Delta G_{bind}$'s into the contributions of electrostatic interactions (EL), van der Waals interactions (VDW), bonds, angles and dihedrals (BADH) and the correction term from change of bond length in the calculations. The results were listed in Table 6.

There is a large negative EL contribution to the $\Delta\Delta G_{solv}$ of desoxy→alcohol. This is obviously related to the increased polarity and hydrogen binding potential of the alcohol inhibitor compared with the desoxy inhibitor. In contrast, the EL contribution to the $\Delta\Delta G_{solv}$ of alcohol→diol is positive, indicating that the electrostatic interactions of the diol inhibitor with water are not better than those of the alcohol inhibitor. This explains why the solubility of the diol inhibitor is not better than that of the alcohol inhibitor.

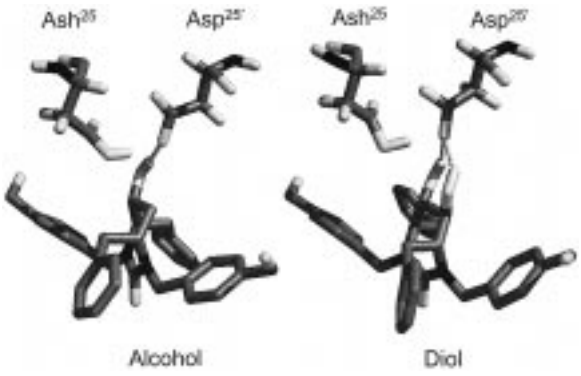


*Figure 5.* The hydrogen bond interactions in the complexes of alcohol and diol inhibitors with the protease in the singly protonated state. $Asp^{25}$ is protonated at the $O_1$ position.

For the binding free energy differences between the inhibitors, both EL and VDW contributions seem to be important, while the contributions from BADH are small. The correction terms of change of bond length is also related to the EL and VDW contributions since it measures the difficulty of stretching the bond length from that of C-H to that of C-O. For desoxy→alcohol, the EL contributions are on average more negative than those of alcohol→diol, while the VDW contributions are on average less positive than those of alcohol→diol. This roughly explains the increased binding affinity for desoxy→alcohol. For alcohol→diol, it appears that every favorable EL contribution is roughly offset by an unfavorable VDW contribution. This may be the reason why $\Delta\Delta G_{bind}$ is close to zero or positive for various protonation states and positions. As an example, we analyzed the electrostatic and hydrogen bonding interactions of the alcohol and the diol inhibitors in the active site with a singly protonated state (Figure 5). The OH group of the alcohol inhibitor can form a hydrogen bond with $Asp^{25'}$. The second OH group of the diol inhibitor can form another hydrogen bond with $Asp^{25'}$. But the two OH groups will repel each other in forming hydrogen bonds with the same oxygen of $Asp^{25'}$. In addition, the OH group of $Asp^{25}$ and the second OH group of the diol inhibitor will repel each other. As

*Table 6.* The contributions of various interactions to $\Delta\Delta G_{bind}$'s and $\Delta\Delta G_{solv}$'s of the inhibitors (in kcal/mol)[a]

| Solvation | Nonol → Alcohol | | | | Alcohol → Diol | | | |
|---|---|---|---|---|---|---|---|---|
| | EL | VDW | BADH | CORC | EL | VDW | BADH | CORC |
| | −7.3 | 2.1 | 0.1 | 0.6 | 0.8 | 0.5 | 0.2 | 0.1 |
| Binding | | | | | | | | |
| (1) Dianionic | −7.1 | 0.7 | 0.0 | 1.2 | −3.8 | 3.6 | −0.2 | 2.6 |
| (2) Single H | | | | | | | | |
| 25′-$O_2$ | −4.5 | 4.4 | 0.0 | 2.5 | −3.4 | 4.0 | −0.2 | 1.8 |
| 25′-$O_1$ | 1.4 | −2.1 | 0.0 | 0.3 | −1.2 | 0.8 | −0.2 | 0.4 |
| 25-$O_2$ | −3.9 | 1.7 | 0.0 | 0.8 | −4.0 | 3.6 | −0.1 | 1.1 |
| 25-$O_1$ | −5.5 | 2.0 | 0.1 | 0.8 | 0.3 | 1.5 | 0.0 | 0.5 |
| (3) Double Hs 25-$O_2$, 25′-$O_2$ | 1.3 | 0.1 | 0.0 | 0.4 | 0.3 | 3.2 | 0.0 | 0.9 |
| 25-$O_1$, 25′-$O_2$ | −4.1 | 1.0 | 0.0 | 0.7 | −0.6 | 2.9 | 0.0 | 0.6 |
| 25-$O_2$, 25′-$O_1$ | −1.8 | 1.1 | 0.0 | 0.3 | −0.2 | 0.7 | −0.1 | 0.8 |
| 25-$O_1$, 25′-$O_1$ | −4.2 | 1.2 | 0.0 | 0.4 | 0.2 | 1.8 | 0.1 | 0.4 |

[a]EL, VDW, BADH and CORC are electrostatic, van der Waals, bonds, angles and dihedrals and correction term due to change of bond length, respectively.

a result, the second OH group of the diol inhibitor does not necessarily help to improve the electrostatic interactions with the protease. From Table 6, in this protonation position, the EL contribution to the $\Delta\Delta G_{bind}$ of desoxy→alcohol is −5.5 kcal/mol, while the EL contribution to the $\Delta\Delta G_{bind}$ of alcohol→diol is +0.3 kcal/mol, in agreement with the structural analysis. It is noted that in different protonation states or protonation positions, the contributions of various interactions are different and obviously the EL, VDW and CORC contributions are strongly coupled to each other.

Our study illustrates the difficulty of ranking of the binding affinities of HIV-1 protease inhibitors. There are three possible protonation states of the two catalytic aspartic acids, i.e., the dianionic, singly protonated and doubly protonated states; the singly and doubly protonated states each may have four protonation positions. To estimate the binding free energy differences between the inhibitors, the protonation states and protonation positions of the complexes and their $pK_a$'s need to be accurately determined. This is because the difference in one $pK_a$ unit corresponds to 1.4 kcal/mol at room temperature and as a result, the error in calculations of $pK_a$'s can greatly influence the accuracy of calculations of the binding free energies of the inhibitors. The determination of the protonation states and protonation positions from experiments such as X-ray crystallography or NMR are difficult because it involves the determination of the exact positions of protons. On the other hand, theoretical calculations of $pK_a$'s by the continuum electrostatics method are also not accurate because of the uncertainty in choosing the dielectric constant inside the protease. In principle, free energy perturbation calculations may be more accurate to determine the $pK_a$'s and protonation positions if long-range interactions are properly included [47]. However, such calculations are very expensive and to achieve the required accuracy is still a challenging task. Although in this study, we were able to predict the trend of the binding affinities of the three forms of DMP323 based on the calculated free energies and the estimated $pK_a$'s from the continuum electrostatics calculations, to calculate the binding free energy differences of the inhibitors, accurate determination of the protonation states and protonation positions are necessary. This remains a significant challenge for HIV-1 protease and related problems.

## Acknowledgements

This work has been supported by NIH grant GM-56531 (P. Ortiz de Montellano, P.I.) to PAK. Supercomputing time was provided by the National Science Foundation at its Supercomputer Centers (Pittsburgh, San Diego, Illinois). The facilities of the UCSF computer graphics laboratory, supported by NIH P41-RR01081, T. Ferrin, P.I., are gratefully acknowledged.

## References


1. Debouck, C., AIDS Res. Human Retroviruses, 8 (1992) 153.
2. Katz, R.A. and Skalka, M., Ann. Rev. Biochem., 63 (1994) 133.
3. Weiss, R.A., Science, 260 (1993) 1273.
4. Johnston, M.I. and Hoth, D.E., Science, 260 (1993) 1286.
5. Suguna, K., Padlan, E.A., Smith, C.W., Carlson, W.D. and Davies, D.R., Proc. Natl. Acad. Sci., 84 (1987) 7009.
6. Wlodawer, A., Miller, M., Jaskolski, M., Sathyanarayana, B.K., Baldwin, E., Weber, I.T., Selk, L.M., Clawson, L., Schneider, L. and Kent, S.B.H., Science, 245 (1989) 616.
7. Wlodawer, A. and Vondrasek, J., Ann. Rev. Biophys. Biomol. Struct., 27 (1998) 249.
8. Thaisrivongs, S., Annu. Rep. Med. Chem., 29 (1994) 133.
9. Boehme, R.E., Borthwick, A.D. and Wyatt, P.G., Ann. Rep. Med. Chem., 30 (1995) 139.
10. Hoetelmans, R.M., Meenhorst, P.L., Mulder, J.W., Burger, D.M., Koks, C.H. and Beijnen, J.H., Pharm. World Sci., 19 (1997) 159.
11. Lam, P.Y.S., Jadhav, P.K., Eyermann, C.J., Hodge, C.N., Ru, Y., Bacheler, L.T., Meek, J.L., Otto, M.J., Rayner, M.M., Wong, Y.N., Chang, C.H., Weber, P.C., Jackson, D.A., Sharpe, T.R. and Erickson-Viitanen, S., Science, 263 (1994) 380.
12. Sham, H.L., Zhao, C., Stewart, K.D., Betebenner, D.A., Lin, S., Park, C.H., Kong, X.P., Rosenbrook, J.W., Herrin, T., Madigan, D., Vasavanonda, S., Lyons, N., Molla, A., Saldivar, A., Marsh, K.C., McDonald, E., Wideburg, N.E., Denissen, J.F., Robins, T., Kempf, D.J., Plattner, J.J. and Norbeck, D.W., J. Med. Chem., 39 (1996) 392.
13. Jorgensen, W.L., Chandrasekhar, J., Madura, J.D., Impey, R.W. and Klein, M.L., J. Chem. Phys., 79 (1983) 926.
14. Pearlman, D.A., Case, D.A., Caldwell, J.W., Ross, W.S., T.E.C. III, Ferguson, D.M., Seibel, G.L., Singh, U.C., Weiner, P. and Kollman, P.A., AMBER, version 4.1, (1995) University of California at San Francisco.
15. Cornell, W.D., Cieplak, P., Bayly, C.I., Gould, I.R., Merz, K.M., Ferguson, D.M., Spellmeyer, D.C., Fox, T., Caldwell, J.W. and Kollman, P.A., J. Am. Chem. Soc., 117 (1995) 5179.
16. Bayly, C.I., Cieplak, P., Cornell, W.D. and Kollman, P.A., J. Phys. Chem., 97 (1993) 10269.
17. Frisch, M.J., Trucks, G.W., Schlegel, H.B., Gill, P.M.W., Johnson, B.G., Robb, M.A., Cheeseman, J.R., Keith, T., Petersson, G.A., Montegomery, J.A., Rahavachari, K., Al-Laham, M.A., Zakrzewski, V.G., Ortiz, J.V., Foresman, J.B., Peng, C.Y., Ayala, P.Y., Chen, W., Wong, M.W., Andres, J.L., Replogle, E.S., Gomperts, R., Martin, R.L., Fox, D.J., Binkley, J.S., Defrees, D.J., Baker, J., Stewart, J.P., Head-Gordon, M., Gonzalez, C. and Pople, J.A., Gaussian 94, Revision B.3, (1995) Gaussian Inc., Pittsburg, PA.
18. Ryckaert, J.P., Ciccotti, G. and Berendsen, H.J.C., J. Comput. Phys., 23 (1977) 327–341.
19. Miyamoto, S. and Kollman, P.A., J. Comput. Chem., 13 (1992) 952.
20. Berendsen, H.J.C., Postma, J.P.M., van Gunsteren, W.F., DiNola, A. and Haak, J.R., J. Chem. Phys., 81 (1984) 3684.
21. Åqvist, J., Medina, C. and Samuelsson, J.-E., Protein Eng., 7 (1994) 385-391.
22. Hansson, T. and Aqvist, J., Protein Eng., 8 (1995) 1137.
23. Chong, L.T., Y., D., Wang, L., Massova, I. and Kollman, P.A., Proc. Nat. Acad. Sci. USA, 96 (1999) 14330.
24. Jayaram, B., McConnell, K.J., Dixit, S.B. and Beveridge, D.L., J. Comput. Phys. 151 (1999) 333.
25. Kollman, P.A., Chem. Rev., 93 (1993) 2395.
26. Wang, L. and Hermans, J., J. Chem. Phys., 100 (1994) 9129.
27. Pearlman, D.A. and Kollman, P.A., J. Chem. Phys., 94 (1991) 4532.
28. Dang, LX, Merz, K.M., Jr. and Kollman, P.A., J. Am. Chem. Soc., 111 (1989) 8505.
29. Sun, Y.-C., Veenstra, D.L. and Kollman, P.A., Prot. Eng., 9 (1996) 273.
30. Mark, A.E. and van Gunsteren, W.F., J. Mol. Biol., 240 (1994) 167.
31. Ido, E., Han, H., Kezdy, F.J. and Tang, J., J. Biol. Chem., 266 (1991) 24359.
32. Sharp, K.A. and Honig, B., Ann. Rev. Biophys. Biophys. Chem., 19 (1990) 301.
33. Gilson, M.K., Sharp, K.A. and H., H.B., J. Phys. Chem., 9 (1988) 327.
34. Honig, B. and Nicholls, A., Science, 268 (1995) 1144.
35. Antosiewicz, J., McCammon, J.A. and Gilson, M.K., J. Mol. Biol., 238 (1994) 415.
36. Hine, J. and Mookerjee, P.K., J. Org. Chem., 40 (1975) 292.
37. Hyland, L.J., Tomaszek, J.T.A. and Meek, T.D., Biochemistry, 30 (1991) 8454.
38. Ferguson, D.M., Radmer, R.J. and Kollman, P.A., J. Med. Chem., 34 (1991) 2654.
39. Reddy, M.R., Viswanadhan, V.N. and Weinstein, J.N., Proc. Nat. Acad. Sci. USA, 88 (1991) 10287.
40. Tropsha, A. and Hermans, J., Protein Eng., 5 (1992) 29.
41. Rao, B.G., Tilton, R.F. and Singh, U.C., J. Am. Chem. Soc. 114 (1992) 4447.
42. Reddy, M.R., Varney, M.D., Kalish, V., Viswanadhan, V.N. and Appelt, K., J. Med. Chem., 37 (1994) 1145.
43. Chen, X.N. and Tropsha, A., J. Med. Chemi., 38 (1995) 42.
44. Rao, B.G. and Murcko, M.A., Protein Eng., 9 (1996) 767.
45. E., B.G.-M., Dwyer, J.J., Gittis, A.G., Lattman, E.E., Spencer, D.S. and Stites, W.E., Biophys. Chem., 64 (1997) 211.
46. Yamazaki, T., Nicholson, L.K., Torchia, D.A., Wingfield, P., Stahl, S.J., Kaufman, J.D., Eyermann, C.J., Hodge, C.N., Lam, P.Y.S., Ru, Y., Jadhav, P.K., Chang, C.H. and Weber, P.C., J. Am. Chem. Soc., 116 (1994) 10791.
47. Buono, G.S.D., Figueirido, F.E. and Levy, R.M., Proteins: Struct. Funct. Genet., 20 (1994) 85.